International Journal of Adhesion & Adhesives 32 (2012) 82–88

Contents lists available at SciVerse ScienceDirect

International Journal of Adhesion & Adhesives

journal homepage: www.elsevier.com/locate/ijadhadh

Characterization and modeling the thermo-mechanical cure-dependent properties of epoxy molding compound

M. Sadeghinia *, K.M.B. Jansen, L.J. Ernst

Delft University of Technology, Mekelweg 2, 2628 CD Delft, The Netherlands

ARTICLE INFO

Article history:
Accepted 13 October 2011
Available online 25 October 2011

Keywords:
Epoxy/epoxides
Viscoelastisity
Cure/hardening
Mechanical properties

ABSTRACT

Semi-conductor devices are mostly encapsulated by epoxy molding compound (EMC) materials. During encapsulation stresses are generated due to the curing of the molding compound. Moreover, additional stresses will build up during cooling down from molding to ambient temperature caused by the differences in the coefficient of thermal expansion. These residual stresses add up to the stresses generated during mechanical loading and may lead to product failure.

The viscoelastic properties of the encapsulation material depend highly on temperature and degree of cure. In this paper the thermo-mechanical properties of an epoxy molding compound with and without filler are investigated both experimentally and theoretically. The cure dependent properties of the EMCs, likewise, the cure kinetics, coefficient of thermal expansion and cure shrinkage were measured using a Differential Scanning Calorimetry (DSC) and a GNOMIX high pressure dilatometer. In addition using a Dynamic Mechanical Analyzer (DMA) the time and temperature dependent storage modulus was measured and mastercurves were constructed.

1. Introduction

Thermosetting polymers are widely used in the electronics industries as packaging materials. Typical examples are electrical insulators, conductive adhesives, molding compounds and underfill materials. The reliability of these materials is of great importance, because their failure may lead to the malfunctionality of the whole product.

Failure in microelectronics packaging mostly happens through polymer cracking, interface delamination and thermal fatigue, caused mainly by thermo-mechanical loadings. Temperature changes occurring during operation may result in mechanical stresses in the individual components of microelectronic packages often through mismatches in the coefficients of thermal expansion. Moreover, shrinkage of the resin material during cure will introduce additional internal stresses. These stresses are generally considered to have a negative influence on the reliability of the product. This is expected to become an even greater problem in the future as a result of ongoing miniaturization accompanied with higher power dissipation densities and greater temperature gradients.

Therefore, nowadays investigating the thermo-mechanical properties of thermosetting polymers has become one of the concern issues in electronic packaging. Studies on the mechanical properties and cure models of polymers have been reported, for example, in [1–9]. Lange et al. [1] proposed a rubbery elastic shrinkage model for predicting cure stresses in Epon 828/EDA resin. Yang et al. [2,3] studied the effect of the filler percentage on the rubbery moduli of a series of silica spheres filled epoxy resins. He showed that most of the modulus built-up occurred during the last 10% of conversion. He also modeled the effect of the filler concentration and curing process on the changes of the rubbery modulus. Also Jansen et al. [4] monitored the changes in viscoelastic properties during cure for commercial molding compounds. Using a specially developed shear tool, he extracted a full cure dependent visco-elastic model for the shear modulus of these materials. Furthermore, Lapique and Redford [5] investigated the characterization of an araldite adhesive with respect to the curing temperature and time. They observed that during the curing process the properties of the adhesive changed drastically. In addition, Preu and Mengel [6] studied the curing behavior of a commercially available adhesive, based on an epoxy compound, by means of dielectric analysis (DEA) and differential scanning calorimetry (DSC). Their results revealed that both measuring methods gain important information for characterizing the curing system, although different kinetic models were found. They also showed that with the DEA method, it was possible to determine an optimal curing temperature for the adhesive. Furthermore, Lu and Wong [7] investigated the changes in thermo-mechanical properties of an isotropic conductive adhesive (ICA) during cure.

* Corresponding author. Tel.: +31 152785707; fax: +31 1582150.
E-mail address: M.sadeghinia@tudelft.nl (M. Sadeghinia).

0143-7496/$ - see front matter © 2011 Elsevier Ltd. All rights reserved.
doi:10.1016/j.ijadhadh.2011.10.007

Curing non-isothermally by a temperature increase from 30 to 250 °C, they studied the heat flow, storage modulus, dimension change and electrical conductivity with a differential scanning calorimeter (DSC), rheometer, thermomechanical analyzer (TMA) and electrical multimeter, respectively. They showed that all of these properties changed dramatically over the same small range of temperature. They also investigated the changes in these four properties with time in the course of an isothermal curing of ICA and revealed that all of the properties change significantly within the same period of time. Chambers et al. [8] investigated the residual stress build-up in thermoset films cured above their glass transition temperature (T_g) and indicated that the residual stress level induced in curing above T_g depends much on the materials. Moreover, Da Silva and Adams [9] investigated the stress-free temperature on the sandwich specimens of CFRP–adhesive–aluminum. Thermal cycling of the samples revealed that for the samples heated above the adhesive's T_g, the thermal stress-free temperature would be T_g of the adhesive. However for heating below it, the curing temperature of the adhesive would be the stress-free temperature.

In this paper an investigation on the thermo-mechanical properties of an epoxy molding compound with and without filler is done. The cure dependent properties of the EMCs, the cure kinetics, the coefficient of thermal expansion and the cure shrinkage were measured through different experiments and the results fitted to models. Also the effect of the filler on the mechanical properties of the cured filled and unfilled materials was considered.

2. Experiments

Different aspects of the mechanical and thermal properties of the molding compounds were measured through a Differential Scanning Calorimetry (DSC), a GNOMIX high pressure dilatometer (PVT) and a Dynamic Mechanical Analyzer (DMA) Apparatus.

Generally, the DSC test reveals T_{g0}, which is T_g of the uncured materials, T_g of the cured materials, the released heat due to the curing and the reaction kinetics, which provides the relation between conversion (degree of cure) and the cure time. Using the PVT, the thermal expansion, cure shrinkage and bulk modulus of the materials can be obtained. The DMA tests are used to determine T_g, glassy and rubbery moduli and the viscoelastic behavior of different materials.

2.1. Materials and sample preparation

The material used for this study is a particulate-filled composite containing similar components as used in commercial molding compounds. The system consists of epoxy Novolac (EPN 1180, Huntsman Advanced Materials, equivalent weight 175–182 g/eq) as a matrix material, Bisphenol-A (equivalent weight 114 g/eq) as hardener and fused silica spheres (FB-940, ex Denka, median diameter 15 μm, density 2.20 g/cm^3) as filler. Triphenylphosphine (TPP, 0.5 g/100 g epoxy) is used as a catalyst. The epoxy Novolac and Bisphenol-A were mixed in a stoichiometric ratio. Two materials were used in these experiments. The unfilled (with 0% filler) and the filled one with 64.5 wt% (50 vol%) filler.

2.2. DSC experiment

2.2.1. Cure kinetics

Differential Scanning Calorimetry (DSC) was used to obtain curing process parameters, such as the degree and rate of chemical conversion and the glass transition temperature. The experiments were performed with a calorimeter of TA-instruments DSC2920 on samples of approximately 5–10 mg in weight. With this device the reaction heat can be detected and related to the degree of conversion (α). The degree of conversion was modeled with the autocatalytic Kamal–Sourour equation [10]:

$$\frac{d\alpha}{dt} = k_0 \exp\left[\frac{-E_a}{RT}\right]\alpha^m(1-\alpha)^n \quad (1)$$

where α is the degree of conversion, R the universal gas constant, 8.314 J/(mol K), T the temperature in Kelvin and E_a the activation energy.

The unknown parameters m and n as well as k_0 and E_a were determined by analyzing temperature scans on non-reacted materials from 0 to 200 °C at heating rates of 5, 10 and 15 °C/min [11] (Table 2).

Fig. 1 shows the measured heat flow with respect to the time in different heating rates for unfilled material. Similar trend is observed for the filled one. The area below the graphs at each time is related to the released heat. The total amount of released heat i.e. H_{tot} is calculated and indicated in Table 1. As it shows H_{tot} in different heating rates is almost constant for filled and unfilled materials separately. However the peak of the released heat increases with increasing heating rates. This is because for a faster heating rate, less time is available to reach a certain temperature and so less time for reaction, resulting in a lower conversion.

As an additional check we estimated the reaction heat for the filled sample, based on that for the unfilled samples and the known filler content (64.5 wt%), assuming that the filler is inert and does not contribute to the released heat. The last row of Table 1 shows that this assumption is indeed justified.

The predicted results for the reaction kinetics based on Eq. (1) and the scan rate experiments discussed above are shown in Fig. 2 as the full lines. Results show that the reaction is much slower in filled materials. It takes about 23 min at 120 °C, for the unfilled material, to reach 60% conversion whereas for the filled material it takes about 117 min to reach this conversion level. This effect

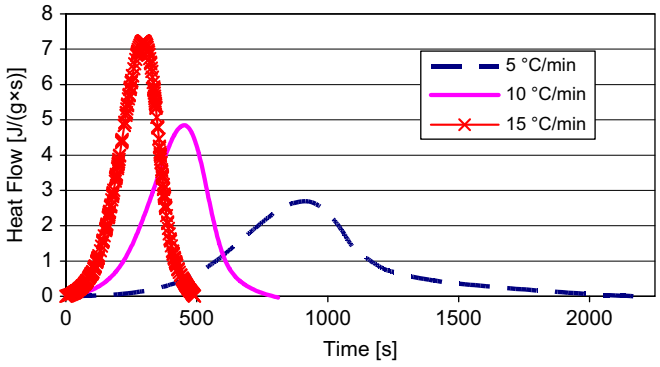

Fig. 1. DSC scanning of uncured unfilled material with different heating rates. The heating rate did not affect the total released heat (see Table 1).

Table 1
H_{tot}, samples cured with different heating rates.

Properties	Rate of heating		
	5 °C/min	10 °C/min	15 °C/min
Released heat, H_{tot}, (J/g), unfilled sample	187	187.1	181.6
Released heat, H_{tot}, (J/g), filled sample	67.8	68	63.3
Calculated H_{tot} (filled sample) based on the H_{tot} of unfilled sample and filler content (J/g)	66.4	66.4	64.5

Table 2
Kinetic parameters of model epoxy system.

Material	E_a (J/mol)	k_0 (s^{-1})	m (–)	n (–)
Unfilled	77.5E3	1.84E7	0.158	1.26
Filled	76.1E3	2.48E6	0.163	1.365

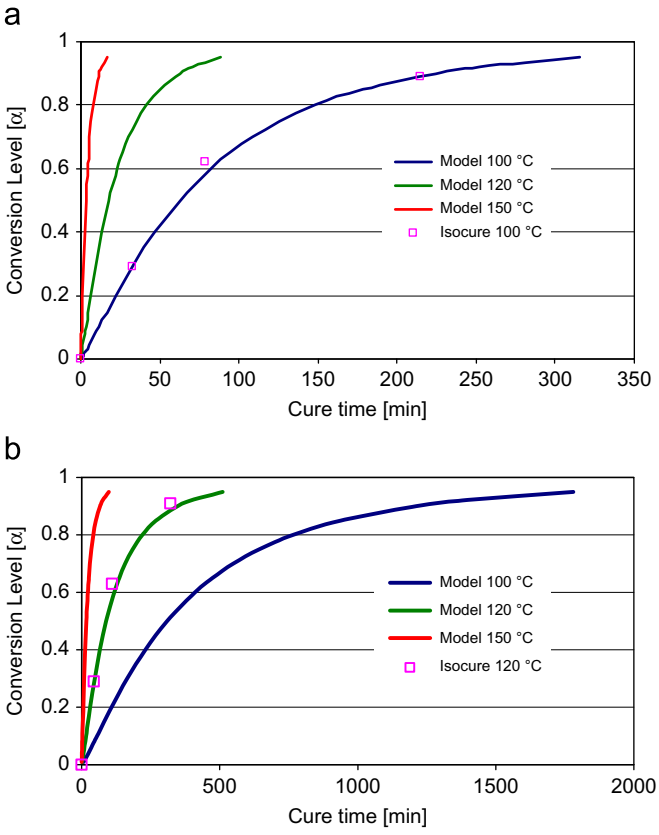

Fig. 2. Conversion vs. curing time at different temperatures. Full lines: prediction for the reaction kinetics; symbols: independent data from isothermal cure experiments; (a) unfilled and (b) filled.

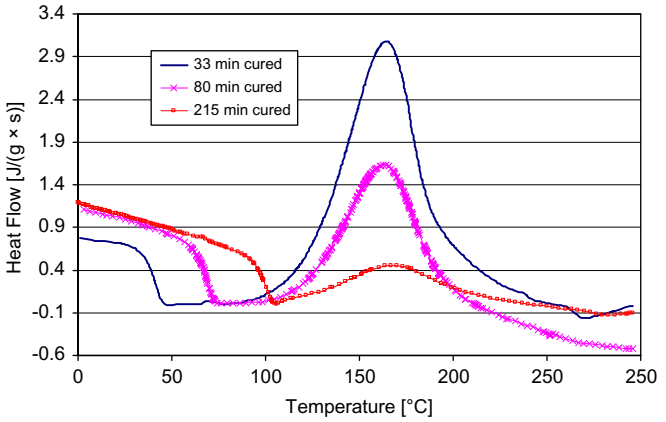

Fig. 3. DSC heat scans of unfilled material partly cured at 100 °C; increasing the conversion level leads to an increase in T_g and a decrease in the released heat.

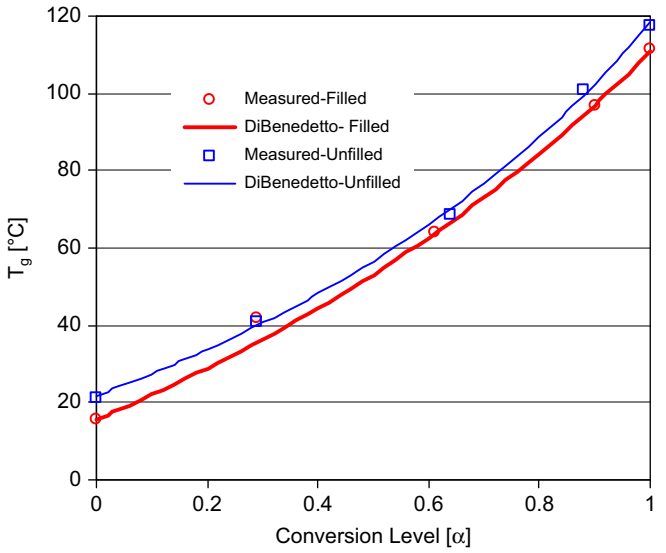

Fig. 4. T_g of partly cured samples; full lines: fit to Eq. (2); symbols: extracted from the heat scan of partially cured samples.

can be interpreted as a partial deactivation of the catalyst by the silica filler.

In order to verify the validity of the reaction kinetics predictions a second, independent method was used. For this purpose we partly cured the materials in the DSC by heating them for a specific time and temperature (100 and 120 °C in this case). These partly cured samples were quickly cooled and subjected to a rescan at 10 °C/min (see Fig. 3). From this rescan the shifted glass transition as well as the remaining heat of reaction could be determined. Based on the latter quantity the conversion could be calculated. These values, as well as the used curing time and temperature, were added to the kinetics predictions in Fig. 2. This shows that there is a good agreement between the conversion predictions and the experimental values from the isothermal cure tests.

2.2.2. Glass transition

The glass transition temperature, indicated as T_g, marks the transition from the glassy (solid) state to the liquid or rubbery state. For polymers this glass transition is not a single temperature but covers a range of about 20–50 °C. There are two T_g values related to each thermoset polymer: T_{g0}, which is related to the uncured material, and T_{g1}, which is related to the fully cured polymer. T_g values can be obtained from DSC data as the change in the slope of the heat flow vs. temperature curve.

The results of the isothermal cure experiments discussed above were used to generate a plot of the glass transition temperature as a function of the conversion level (see Fig. 4). This shows a gradual increase of T_g from about 20 to 120 °C. The curve for the filled material appears to be about 5 °C lower over the whole trajectory.

The glass transition temperature curves were fitted to the empirical DiBenedetto model [12]:

$$T_g(\alpha) = T_{g0} + \frac{(T_{g1} - T_{g0})\lambda\alpha}{1-(1-\lambda)\alpha} \quad (2)$$

where α denotes the degree of cure and λ is a fitting parameter. T_{g0}, T_{g1} and $T_g(\alpha)$ are the glass transition temperatures of uncured, fully cured and partly cured samples, respectively. The parameters obtained from this fit are summarized in Table 3.

2.3. PVT measurement

2.3.1. Cure shrinkage

During cure, the EMC transforms from the liquid state into a visco-elastic solid. The formation of chemical crosslinks leads to a

Table 3
Parameters for Eq. (2).

	T_{g0} (°C)	T_{g1} (°C)	λ
Unfilled	21.4	117.7	0.567
Filled	15.5	111.2	0.652

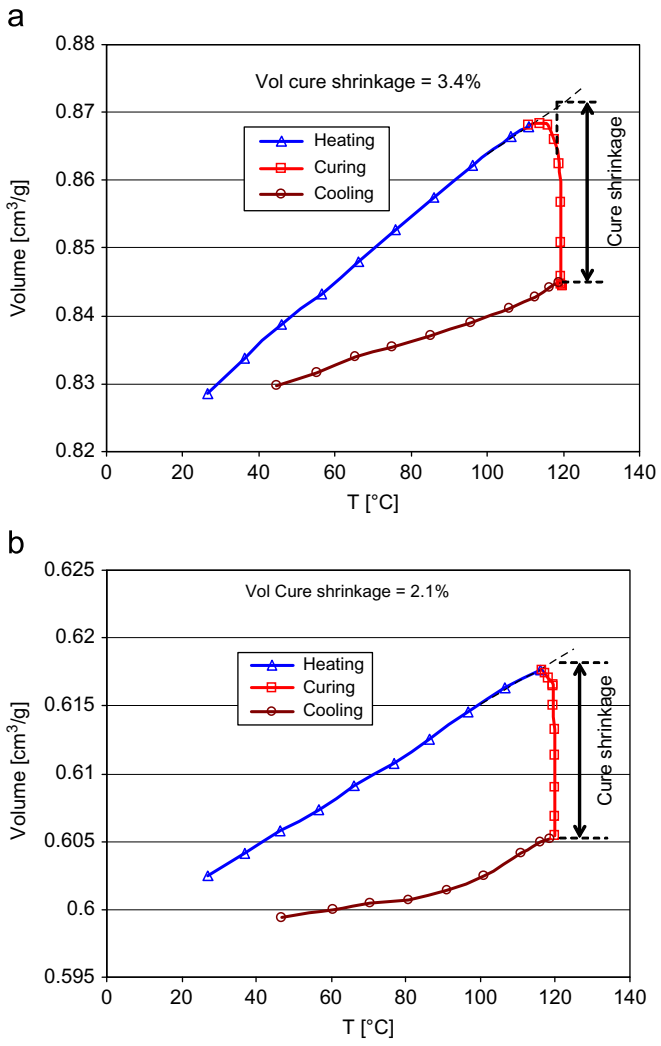

Fig. 5. Volume changes during heating (5 °C/min); cooling and shrinkage during isothermal cure; (a) unfilled and (b) filled.

volumetric shrinkage. This shrinkage contributes for a large extent to the residual stresses in electronic packages. A GNOMIX high pressure dilatometer (PVT Apparatus) was used to determine the amount of volumetric decrease due to the curing.

The experimental cure shrinkage plots for filled and unfilled materials are shown in Fig. 5. The graph is divided into three major parts: increase in volume during heating, subsequent isothermal cure shrinkage and cooling down to room temperature. During heating the material is still unreacted and is in the liquid state, so the thermal expansion is large. After cure, the glass transition temperature is much higher and the material is mostly cooling down in the solid state where the thermal expansion is low.

Although molding of micro-electronic products is performed at 175 °C, in this experiment, a much lower curing temperature (120 °C) is applied in order to slow down the reaction. The kinetic study shows that still 100% conversion is obtained for long enough curing at 120 °C.

During the heating up stage, the sample already starts to cure in the apparatus before reaching the curing temperature. Therefore the volume changes are then caused by both changes in temperature and actual cure shrinkage. To correct this, the thermal contribution is estimated by extrapolating the heating curve (full lines in Fig. 5). The real cure shrinkage is defined as the measured total volume change minus the thermal expansion contribution.

The total cure shrinkage can be calculated from the difference of the values at the end and starting time of the cure. Due to the filler, the cure shrinkage of the filled material is less than the unfilled one (2.1 vs. 3.4 vol%).

The cure shrinkage of the filled material can also be calculated assuming the filler as an inert material and that the shrinkage is only caused by the matrix. The calculated value is 1.7 vol%, which is reasonably close to the measured one i.e. 2.1 vol%.

Replacing the curing time with conversion (using Eq. (1) and Fig. 2), the cure shrinkage can be extracted with respect to the conversion; see Fig. 6. Similar results are observed for the unfilled sample. Since on a molecular level, the cure shrinkage emerges from the reduction in free volume of monomer units, which react to the network, this reduction can be expected to be constant for all reacting units. It is therefore expected that the cure shrinkage is proportional to the conversion. Indeed, Fig. 6 shows that the cure shrinkage's curves are approximately linear. Deviation at low and high conversion levels emerge because in these regimes the kinetic fits are less accurate.

For practical purposes we neglect these deviations and approximate the cure shrinkage as being linear with conversion, Eq. (3). The result of the model is also shown in Fig. 6.

$$\varepsilon_v^{cure} = \alpha\gamma_c \tag{3}$$

where ε_v^{cure} is the volumetric cure shrinkage and γ_c is the volumetric shrinkage at 100% conversion.

2.3.2. Coefficient of thermal expansion (CTE)

The high pressure dilatometer was also used to determine the coefficient of thermal expansion (CTE) of the fully cured EMC. For these measurements the sample pressure and temperature were stepwise increased and the corresponding volume changes were recorded. Typical temperature and pressure ranges were 40–200 °C (in steps of 10 °C) and 10–100 MPa (in steps of 10 MPa), respectively.

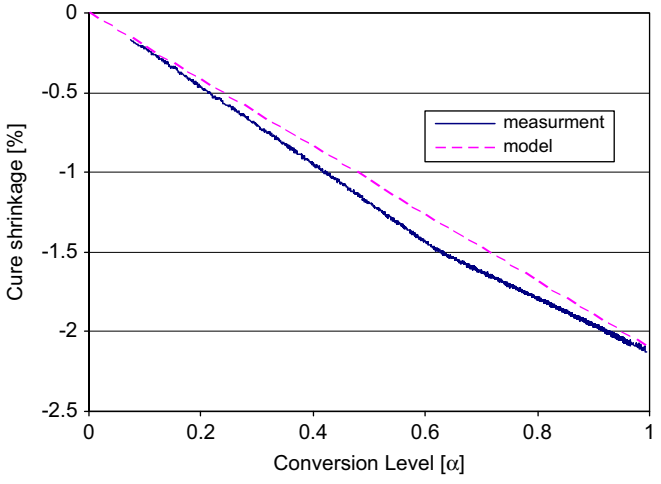

Fig. 6. Cure shrinkage vs. conversion level for the filled sample; full lines: PVT measurement; dashed line: linear approximation to Eq. (3).

The volume change of the fully cured filled molding compounds is shown in Fig. 7. The PVT diagram for the unfilled sample had similar shape and is not shown here.

The results clearly show a linear volume increase in the glassy region and a second linear region above T_g. With respect to the data analysis it is more convenient to fit the volume changes first to a model and then obtain the coefficients of thermal expansion and the compressibility by differentiating this model with respect to temperature and pressure, respectively. As a model we use the well known Tait equation [13]:

$$\upsilon(T,P) = \upsilon''(T)\left[1 - C\ln\left(1 + \frac{P}{b_1 \exp(-b_2 T)}\right)\right] \tag{4}$$

where $C=0.0894$ and b_1 and b_2 are the fitting parameters. In order to allow for a smooth transition between glassy and rubbery behaviors we modified the thermal part $\upsilon''(T)$ as

$$\upsilon''(T) = \upsilon_0\left(1 + k_1(T - T_{gp}) + \frac{1}{2}k_2\left[(T - T_{gp}) + \frac{\ln(\cosh[A_1(T - T_{gp})])}{A_1}\right]\right) \tag{5}$$

in which A_1 is a fitting parameter related to the width of the transition regime and T_{gp} is the pressure dependent glass transition temperature $T_{gp} = T_g^{pvt} + s_0 P$.

Here T_g^{pvt} is the fully cured T_g at atmospheric pressure and s_0 is a fitting parameter. The fit parameters were determined by non-linear curve fitting (using MatLab) and are summarized in Table 4. As mentioned before, the volumetric CTE then follows by differentiating with respect to temperature, resulting in

$$CTE_v(T,0) = k_1 + \tfrac{1}{2}k_2(1 + \tanh[A_1(T - T_g^{pvt})]) \tag{6}$$

Since the tanh function varies between -1 and $+1$, k_1 and (k_1+k_2) represent the volumetric thermal expansion in the rubbery and glassy states, respectively.

Since it is more customary to work with the linear coefficients of thermal expansion we defined those as 1/3 of the volumetric ones. The linear coefficients of thermal expansion are presented in Fig. 8.

This shows that the glassy and rubbery CTE of the filled samples is almost 45% of that of the unfilled sample, which matches quite well with expectation since the expansion is mostly due to the resin, which is almost 50 vol% of the filled materials' contents.

Table 4 shows that for the unfilled material there is not that much difference compared with T_g values obtained from PVT measurement to DSC (Table 3). However, there is a difference between these values for the filled ones: 111.2 °C for DSC and 98 °C for PVT. Such differences are because the glass transition is a kinetic process, which takes place in a certain temperature and time range. It therefore depends on both the measurement method and the data evaluation procedure.

2.3.3. Compressibility and bulk modulus

The compressibility is a fundamental material property that relates the volume change in a material to the imposed hydrostatic stress. This property can be determined in a similar way as for the CTE but now by differentiating with respect to volume:

$$\beta(T) = k_1 s_0 + \frac{1}{2}k_2 s_0\left\{1 + \tanh\left[A_1(T - T_g^{pvt})\right]\right\} + \frac{C}{b_1 \exp(-b_2 T)} \tag{7}$$

The bulk modulus is a material property, which is often needed as input in most thermal–mechanical simulation software and is obtained here as the inverse of the bulk compressibility:

$$K = \frac{1}{\beta(T)} \tag{8}$$

Fig. 9 shows that as expected both the glassy and rubbery bulk moduli increase with filler content. Due to filler the glassy and rubbery bulk moduli of the filled sample become, respectively, 2.4 and 2 times higher than unfilled one.

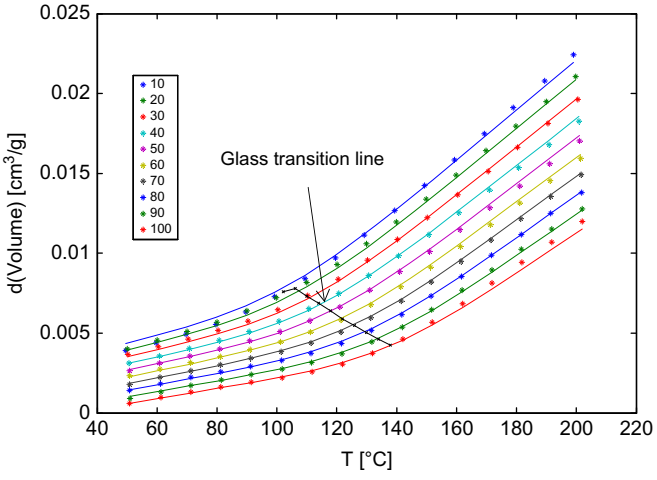

Fig. 7. Volume changes for filled material in different temperature and pressure from PVT measurement; symbols: experimental data; full lines: fit to Eq. (5); the legend refers to the applied pressures.

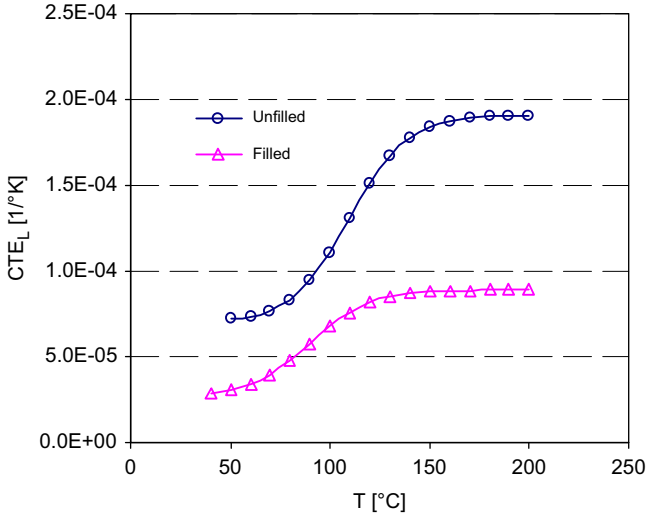

Fig. 8. Linear CTE of unfilled and filled materials vs. temperature, extracted from the PVT measurement.

Table 4
T_g and fit parameters corresponding to Eqs. (4) and (5); $C=0.0894$.

Material	Properties							
	υ_0 (cm³/gm)	k_1 (1/°C)	k_2 (1/°C)	A_1 (1/°C)	b_1 (MPa)	b_2 (1/°C)	T_g^{pvt} (°C)	s_0 (°C/MPa)
Unfilled	0.846	2.1E−4	3.63E−4	0.035	1370.9	6.4E−3	109.7	0.324
Filled	0.609	7.9E−5	1.88E−4	0.033	5633.8	9.1E−3	98	0.445

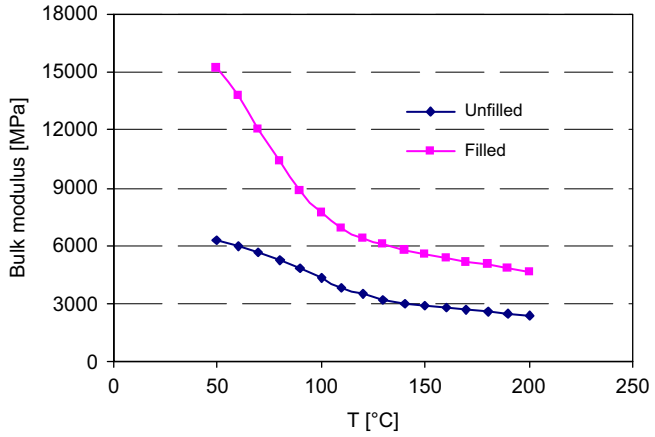

Fig. 9. Bulk modulus of unfilled and filled materials in different temperatures. Data are extracted from the PVT measurement.

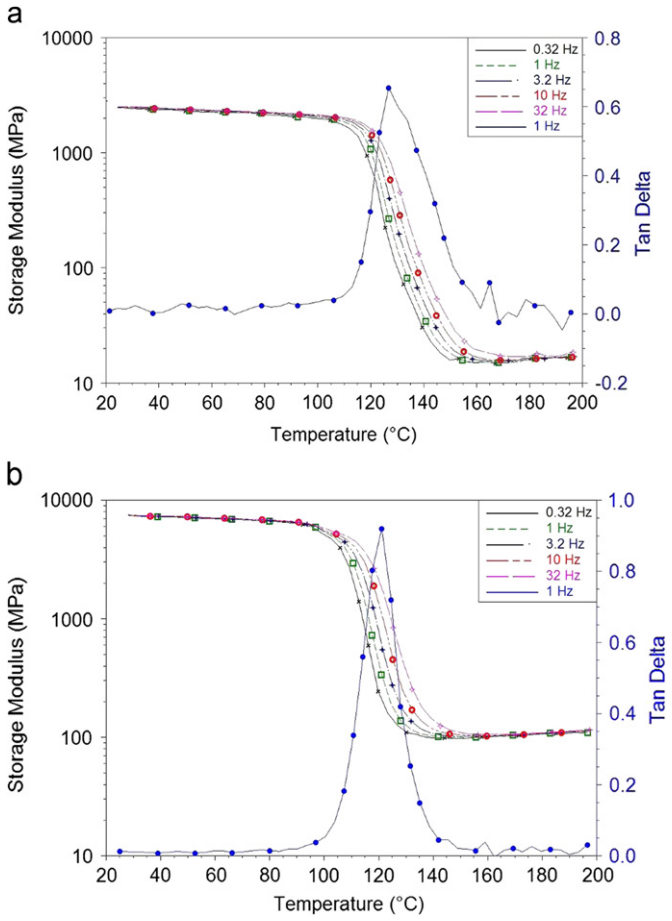

Fig. 10. Storage modulus (E'') vs. temperature measured by the DMA experiment: (a) unfilled material and (b) filled material. The tan δ curve is only shown for 1 Hz frequency.

2.4. Dynamic Mechanical Analyzer (DMA)

A Dynamic Mechanical Analyzer, TA Q800, was used to measure the viscoelastic elongation behavior of filled and unfilled fully cured samples as a function of the excitation frequency and temperature. The samples had the dimension of $22.6 \times 4.9 \times 0.5\ mm^3$ and $22.5 \times 5.0 \times 0.9\ mm^3$, for filled and unfilled, respectively. The experiments covered the frequency and temperature range of 0.32–32 Hz and 20–200 °C, respectively.

Fig. 10 clearly shows that for each material, E_g (Elongation glassy modulus) and E_r (Elongation rubbery modulus) are independent of the frequency. However in the glass transition regime clear frequency dependent effects can be seen. If we take the peak position of 1 Hz tan δ curves as the DMA glass transition temperature, we obtain values of 128 °C and 121 °C for the unfilled and filled material, respectively. As the glass transition temperature is dependent on the type of experiment (Section 2.3.2), these values are larger than the dilatometric and the DSC data.

Table 5 shows that, due to the usage of filler, E_g and E_r of the filled materials are almost 3.2 and 6.4 times more than those of the unfilled materials, respectively. Further, T_g of the unfilled material is more than the filled one.

Table 5
Glassy, rubbery modulus and T_g, according to DMA test, T_g values at 1 Hz.

Material	Properties			
	Glassy modulus (MPa)	Rubbery modulus (MPa)	T_g (E'') (°C)	T_g (tan δ) (°C)
Unfilled	2253	16.3	121.3	128
Filled	7239	108.3	112.5	121

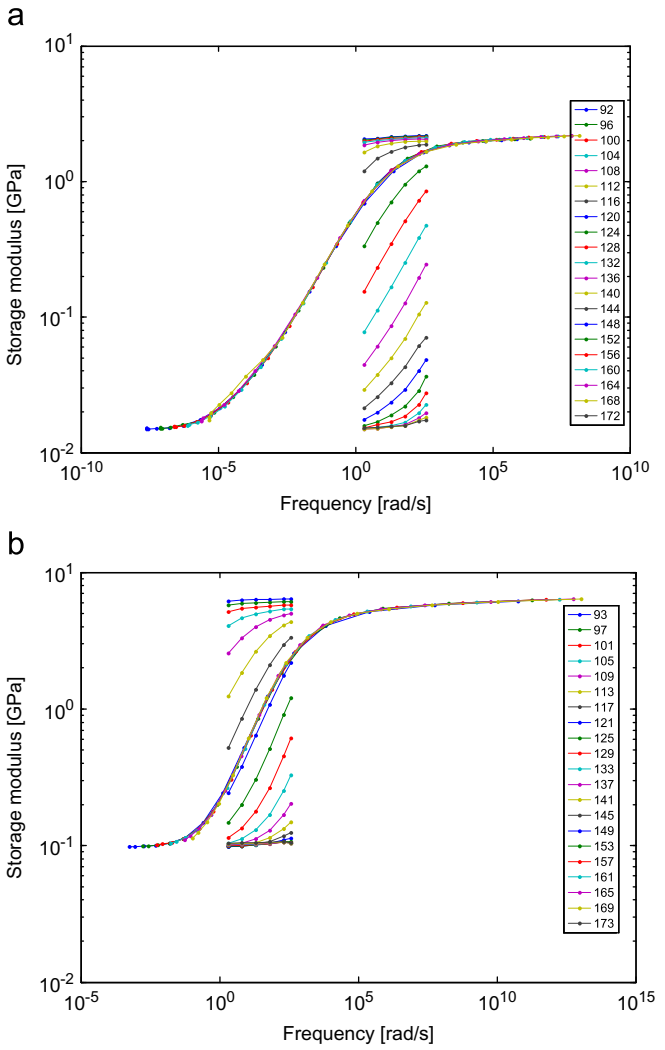

Fig. 11. Storage modulus (E'') and viscoelastic elongation modulus mastercurve as a function of frequency; data extracted by analyzing the DMA elongation measurements; T_{ref}=120 °C; (a) unfilled and (b) filled.

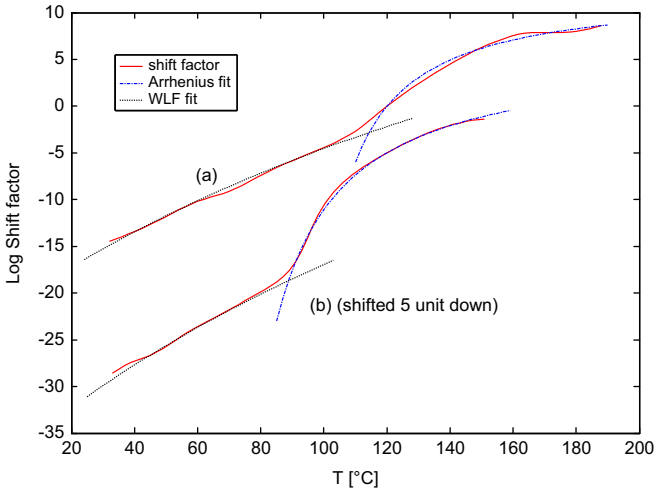

Fig. 12. Shift factors related to the elongation mastercurve. Details of Arrhenius and WLF fit to the fully cured shift factor curve; (a) unfilled and (b) filled; T_{ref}=120 °C. The filled sample curve was shifted 5 units down for clarity.

Table 6
WLF and the Arrhenius fit parameters for temperature shift factors. T_{ref}=120 °C.

Material	C_1	C_2	T_g^{DMA} (°C)	H (kJ/mol)	T_0 (K)	T_c (°C)
Unfilled	12.56	31.03	131.3	331	140.5	114
Filled	11.1	56.6	126.4	401	200.5	90

The storage modulus can be interpolated and plotted as a function of frequency and temperature, Fig. 11. Time–temperature superposition appears to be valid for the fully cured filled and unfilled materials. The shift factors a_T are determined from the storage modulus curve and plotted in Fig. 12, using T=120 °C as the reference temperature. A marked change in the slope of a_T close to the glass transition temperature is observed in this figure, which is attributed to a change in relaxation mechanism. Below the switching temperature, T_c, the shift factor follows the Arrhenius behavior [14] (activation energy driven), Eq. (9), whereas above this temperature it follows the WLF behavior [15] (free volume mechanism), Eq. (10). The corresponding parameters related to shift factor are summarized in Table 6. The models with the estimated parameters were also plotted in Fig. 12 and a good fit in the measured domain was observed.

$$\log a_T^{\mathrm{Arrh}} = \frac{-H}{2.30R}\left(\frac{1}{T}-\frac{1}{T_0}\right), \quad T < T_c \tag{9}$$

$$\log a_T^{\mathrm{WLF}} = \frac{C_1(T-T_{\mathrm{ref}})}{C_2+T-T_{\mathrm{ref}}}, \quad T > T_c \tag{10}$$

3. Conclusions

In this paper an extensive study on the thermo-mechanical cure-dependent properties of a series of epoxy resins with and without filler was carried out. Using the Differential Scanning Calorimetry and a GNOMIX high pressure dilatometer the cure kinetics, coefficient of thermal expansion and cure shrinkage were measured. In addition using a Dynamic Mechanical Analyzer the viscoelastic storage modulus was measured and applying the Time–Temperature Superposing principle, the master-curves were extracted. The effect of the filler was also investigated on these thermo-mechanical properties and the result shows that the filler decreases the cure shrinkage and thermal contraction of epoxy resins but increases the modulus below and above the glass transition temperature.

Acknowledgments

We thank the European Commission for funding this work in FP7 under project NanoInterface (NMP3-SL-2008-214371).

References

[1] Lange J, Toll S, Manson JE, Hult A. Residual stress build-up in thermoset films cured above their ultimate glass transition temperature. J Polym 1995;36(16):3135–41.
[2] Yang DG. Cure-dependent viscoelastic behaviour of electronic packaging polymers. PhD thesis. Delft; 2007.
[3] Yang DG, Jansen KMB, Ernst LJ, Zhang GQ, Bressers HJL, Janssen JHJ. Effect of filler concentration of rubbery shear and bulk modulus of moulding compounds. J Microelectron Reliab 2007;47:233–9.
[4] Jansen KMB, Qian C, Ernst LJ, Bohm C, Kessler A, Preu H, et al. Modelling and characterization of moulding compound properties during cure. J Microelectron Reliab 2009;49:872–6.
[5] Lapique F, Redford K. Curing effects on viscosity and mechanical properties of a commercial epoxy resin adhesive. Int J Adhes Adhes 2002;22:337–46.
[6] Preu H, Mengel M. Experimental and theoretical study of a fast curing adhesive. Int J Adhes Adhes 2007;27:330–7.
[7] Lu D, Wong CP. Effects of shrinkage on conductivity of isotropic conductive adhesives. Int J Adhes Adhes 2000;20:189–93.
[8] Chambers RS, Lagasse RR, Guess TR, Plazek DJ, Bero C. A rubbery cure shrinkage model for analyzing encapsulated assemblies. J Electron Package 1995;117(3):249–54.
[9] Da Silva LFM, Adams RD. Stress-free temperature in a mixed-adhesive joint. J Adhes Sci Technol 2006;20:1705–26.
[10] Sourour S, Kamal MR. Differential scanning calorimetry of epoxy cure: isothermal cure kinetics. Thermochim Acta 1976;14(1):41–59.
[11] Turi A. Thermal characterization of polymeric materials, 2nd ed. San Diego: Academic Press; 1997.
[12] Cheng SZD. Handbook of thermal analysis and calorimetry, vol. 3: application to polymers and plastics. Amsterdam: Elsevier Science; 2002.
[13] Simha R, Wilson PS, Olabisi O. Pressure–volume–temperature properties of amorphous polymers—empirical and theoretical predictions. Kolloid Z Z Polym 1973;251(6):402–8.
[14] McNaught AD, Wilkinson A. Compendium of chemical terminology, 2nd ed. Oxford: IUPAC Blackwell Scientific; 1997.
[15] Williams ML, Landel RF, Ferry JD. The temperature dependence of relaxation mechanisms in amorphous polymers and other glass-forming liquids. J Am Chem Soc 1955;77:3701–7.